1988

Oxygen Reduction on Silver in 6.5M Caustic Soda Solution

Prosper K. Adanuvor
Texas A & M University - College Station

Ralph E. White
University of South Carolina - Columbia, white@cec.sc.edu

Publication Info

Journal of the Electrochemical Society, 1988, pages 2509-2517.

REFERENCES

1. A. Ennaoui, S. Fiechter, W. Jaegermann, and H. Tributsch, *This Journal*, **133,** 97 (1986).
2. W. Jaegermann and H. Tributsch, *J. Appl. Electrochem.*, **13,** 743 (1983).
3. S. B. Lalwani and M. Shami, *This Journal*, **133,** 1364 (1986).
4. C. A. Vincent, "Modern Batteries," p. 182, Edward Arnold Ltd., London (1984).
5. T. Biegler and D. A. Swift, *Electrochim. Acta*, **24,** 415 (1979).
6. D. F. A. Koch, in "Modern Aspects of Electrochemistry," Vol. 11, J. O'M. Bockris and B. E. Conway, Editors, p. 211, Plenum Press, New York (1975).
7. R. T. Lowson, *Chem. Rev.*, **82** (5), 461 (1982).
8. R. A. Meyers, "Coal Desulfurization," Marcel Dekker Inc., New York (1977).
9. E. Peters and H. Majima, *Can. Met. Quart.*, **7,** 111 (1968).
10. L. K. Bailey and E. Peters, *ibid.*, **15,** 333 (1976).
11. T. Biegler, *J. Electroanal. Chem.*, **70,** 265 (1976).
12. T. Biegler, D. A. J. Rand, and R. Woods, *ibid.*, **60,** 151 (1975).
13. K. K. Mishra and K. Osseo-Asare, *Fuel*, **66,** 1161 (1987).
14. O. M. Ogunsola and K. Osseo-Asare, *ibid.*, **65,** 811 (1986).
15. C. Moses, D. Nordstrom, J. Herman, and A. Mills, *Geochimica Cosmochimica Acta*, **51,** 1561 (1987).
16. E. Peters, in "Electrochemistry in Minerals and Metal Processing," P. E. Richardson, S. Srinivasan, and R. Woods, Editors, p. 343, The Electrochemical Society, Softbound Proceeding Series, Pennington, NJ (1984).
17. D. Frost, W. R. Leeder, R. L. Tapping, and B. Wallband, *Fuel*, **56,** 272 (1977).
18. G. Springer, *Trans. Inst. Min. Metall.*, **79C,** 11 (1970).
19. S. R. Morrison, "Electrochemistry at Semiconductor and Oxidized Metal Electrodes," Plenum Press, New York (1980).
20. R. Memming, *Prog. Surf. Sci.*, **17,** 1 (1984).
21. M. Gerischer, *This Journal*, **58,** 263 (1975).
22. H. Tributsch, *Struct. Bonding (Berlin)*, **49,** 127 (1982).
23. H. Tributsch, in "Modern Aspects of Electrochemistry," Vol. 17, J. O'M Bockris, B. E. Conway, and R. G. White, Editors, p. 303, Plenum Press, New York (1986).
24. D. J. Vaughan and J. Craig, "Mineral Chemistry of Metal Sulfides," p. 37, Cambridge University Press, London (1978).
25. D. W. Bullet, J. Phys. C., **15,** 6163 (1983).
26. T. A. Bither, C. T. Prewitt, J. L. Gillson, P. G. Bierstead, and R. B. Young, *Solid State Commun.*, **4,** 533 (1966).
27. R. L. Paul, M. J. Nicol, J. W. Diggle, and A. D. Saunders, *Electrochim. Acta*, **23,** 625 (1978).
28. K. K. Mishra and K. Osseo-Asare, *This Journal*, **135,** 1898 (1988).
29. B. E. Conway, J. C. H. Ku, and F. C. Ho, *J. Colloid Interface Sci.*, **75,** 357 (1980).
30. H. A. Kozlowska, B. E. Conway, and W. B. A. Sharp, *J. Electroanal. Chem.*, **43,** 9 (1973).
31. S. M. Jordanov, H. A. Kozlowska, M. Vukovic, and B. E. Conway, *This Journal*, **125,** 1471 (1978).
32. N. Ramasubramanian, *J. Electroanal. Chem.*, **64,** 21 (1975).
33. F. Johnston and L. Mcamish, *J. Colloid Interface. Sci.*, **42,** 112 (1973).
34. E. T. Seo and D. T. Sawyer, *Electrochim. Acta*, **10,** 239 (1965).
35. A. J. Bard, R. Person, and J. Jordan, "Standard Potential in Aqueous Solutions," pp. 100-111, Marcel Dekker, Inc., New York (1984).
36. D. Lyons and G. Nickless, in "Inorganic Sulfur Chemistry," G. Nickless, Editor, p. 509, Elsevier Pub. Co., Amsterdam (1968).
37. M. Goldhaber, *Am. J. Sci.*, **283,** 193 (1983).
38. M. A. McKibben, Ph.D. Thesis, The Pennsylvania State University, University Park, PA (1984).

Oxygen Reduction on Silver in 6.5*M* Caustic Soda Solution

Prosper K. Adanuvor and Ralph E. White*

Department of Chemical Engineering, Texas A&M University, College Station, Texas 77843

ABSTRACT

The cathodic reduction of oxygen in 6.5*M* membrane-grade caustic soda solution has been studied experimentally at a silver rotating disk electrode at 25°C. The results can be approximated by the parallel mechanism for oxygen reduction with catalytic decomposition of peroxide. Further analysis of this mechanism indicates that the sequential process with catalytic decomposition of peroxide predominates over the direct $4e^-$ process. Direct application of the sequential mechanism to the data indicates that the latter mechanism with catalytic decomposition of peroxide much more accurately reflects the experimental results. The relevant kinetic parameters are calculated on the basis of the mechanisms presented.

Silver shows a reasonably high catalytic activity for oxygen reduction in alkaline electrolytes. Furthermore, it serves as an excellent peroxide decomposition catalyst (1, 2). For this reason, silver has attracted considerable interest as a potential oxygen reduction catalyst in fuel cells (3), metal-air batteries (4), and more recently as a replacement of hydrogen-generating cathodes in the chlor-alkali industry (5).

Oxygen reduction on silver has been investigated by several investigators (6-13). The reduction process has been found to follow two reaction pathways: the direct $4e^-$ path as represented by reaction [1]

$$O_2 + 2H_2O + 4e^- = 4\ OH^- \qquad [1]$$

and the $2e^-$ path (generally referred to as the sequential path) involving the formation of peroxide as an intermediate product (Eq. [2]) with further reduction of peroxide to OH^- by Eq. [3] at higher applied potentials

$$O_2 + H_2O + 2e^- = HO_2^- + OH^- \qquad [2]$$

$$HO_2^- + H_2O + 2e^- = 3\ OH^- \qquad [3]$$

Both the direct $4e^-$ pathway and the sequential pathway have been shown to occur simultaneously on silver (11).

The decomposition of peroxide occurs by the catalytic reaction in Eq. [4]

$$HO_2^- = 1/2\ O_2 + OH^- \qquad [4]$$

To enhance its catalytic activity, silver is used in high surface area forms such as porous electrodes where the silver catalyst is dispersed in the porous matrix. In the porous structure, silver acts as a catalyst for the oxygen reaction and at the same time suppresses the peroxide concentration via reaction [4] to a very low level, thereby extending the operating life of the electrode as well as improving the cell efficiency.

Serious discrepancies exist in the kinetic parameters reported in the literature for oxygen reduction on silver. For example, Fabjan *et al.* (12) reported Tafel slopes of −45 to −50 mV/decade as compared to the value of −150 mV/decade reported by Fischer and Heitbam (11). Similarly, the reported exchange current densities show significant

*Electrochemical Society Active Member.

variations. Similar variations in the kinetic parameters for oxygen reduction on silver have been reported by other investigators as well (10). The discrepancies in the reported values have generally been attributed to the nature of the electrode surface, the different pretreatment of the electrodes, and the condition under which the data are collected (10). Another significant factor contributing to the discrepancies in the reported values that has been neglected until recently, is the fact that the classical techniques for electrochemical data analysis are generally inadequate for the analysis of such complex electrochemical reaction systems because of coupling and interaction of the component reactions or processes with each other. An alternative data analysis technique presented recently by the authors (14) is well suited for analyzing such complex reaction systems.

To date, a significant proportion of the kinetic data in the literature on oxygen reduction on silver has been reported for potassium hydroxide as the electrolytic solution medium (7-13). Very limited data is available for oxygen reduction in caustic soda solutions, and where available, it has been reported for very low caustic concentrations (6, 15). With increasing application of membrane-cell technology to the production of caustic soda, and with the potential application of the oxygen (or air) cathode as a substitute for the hydrogen-generating cathodes currently in use in the chlor-alkali industry, it is important to understand the kinetics of oxygen reduction in strong caustic solutions. The objective of this work is to elucidate the reaction mechanism and to obtain the kinetic parameters for oxygen reduction on silver in 6.5*M* sodium hydroxide solution. This concentration is typical of the caustic soda produced from membrane-cells. Also, alkaline fuel cells and alkaline metal-air batteries normally operate with concentrated solutions of KOH (or NaOH) electrolyte [up to 45 weight percent (w/o)] (3). A concentrated solution of the electrolyte has the advantage of lowering the vapor pressure of the solution and thereby avoiding the operation of the cell at high pressures for water product control. Another advantage of using a concentrated solution of the electrolyte is that the ohmic potential drop in the solution can be reduced appreciably.

Mechanistic Models for Oxygen Reduction

The reduction process involves the transport of oxygen from the bulk solution to the electrode where it is adsorbed on sites at the electrode surface. The peroxide intermediate formed can, in addition to undergoing electrochemical and catalytic decomposition, desorb from the surface to be transported into the bulk solution. Depending on the experimental conditions and the nature of the electrode, the reduction process can occur by a simple reaction step or by a combination of two or more simple reactions as represented by Eq. [1]-[4]. Each simple reaction is made up of a number of elementary steps as postulated in Eq. [1a]-[1d], Eq. [2a]-[2d], Eq. [3a]-[3d], and Eq. [4a]-[4c], respectively. The elementary steps represent the mechanistic process by which the simple reactions occur. M $\cdots$ O indicates the adsorption of a species O on a site M at the electrode surface

$$O_2 + 2H_2O + 4e^- \rightarrow 4\ OH^-$$

$$\begin{cases} O_2 + 2M \rightleftharpoons 2M\cdots O & [1a] \\ 2(M\cdots O + e^- \rightarrow MO^-) & [1b] \\ 2(MO^- + H_2O \rightleftharpoons MOH + OH^-) & [1c] \\ 2(MOH + e^- \rightleftharpoons OH^- + M) & [1d] \end{cases}$$

$$O_2 + H_2O + 2e^- \rightleftharpoons HO_2^- + OH^-$$

$$\begin{cases} O_2 + M \rightleftharpoons M\cdots O_2 & [2a] \\ M\cdots O_2 + e^- \rightarrow MO_2^- & [2b] \\ MO_2^- + H_2O \rightleftharpoons MHO_2 + OH^- & [2c] \\ MHO_2 + e^- \rightleftharpoons HO_2^- + M & [2d] \end{cases}$$

$$HO_2^- + H_2O + 2e^- \rightarrow 3\ OH^-$$

$$\begin{cases} HO_2^- + M \rightleftharpoons MHO_2^- & [3a] \\ MHO_2^- + H_2O \rightleftharpoons MH_2O_2 + OH^- & [3b] \\ MH_2O_2 + e^- \rightarrow MOH + OH^- & [3c] \\ MOH + e^- \rightleftharpoons OH^- + M & [3d] \end{cases}$$

$$2HO_2^- \rightarrow O_2 + 2\ OH^- \quad \begin{cases} HO_2^- + M \rightleftharpoons MHO_2^- & [4a] \\ MHO_2^- \rightarrow MO + OH^- & [4b] \\ MO + HO_2^- \rightarrow O_2 + OH^- + M & [4c] \end{cases}$$

Development of Kinetic Equations for Oxygen Reduction on Ag

The kinetic equations are derived for each simple reaction based on the proposed sequence of elementary steps comprising that reaction. For reaction [1], the direct $4e^-$ reduction of O_2, step [1b] is assumed to be the rate-determining step (rds). The following assumptions were made to facilitate the derivation of the kinetic expression for the current density: (*i*) the rates of the elementary steps prior to and after the rds are high enough to be in quasi-equilibrium, (*ii*) the coverage of the electrode surface by adsorbed species is low, (*iii*) double layer effects are negligible, and (*iv*) the electrolyte behaves as an ideal solution.

The rate expression for the rds in Eq. [1b] can be expressed as

$$\frac{i_1}{n_1\mathbf{F}} = k_b c^2_{MO^-} \exp\left[\frac{n_b\alpha_b\mathbf{F}}{RT}V\right] - k_{-b}c^2_{M\cdots O} \exp\left[-\frac{n_b(1-\alpha_b)\mathbf{F}}{RT}V\right] \quad [5]$$

where V is the potential difference between the electrode and the adjacent solution just beyond the double layer

$$V = \Phi_{met} - \Phi_o \quad [6]$$

Application of the quasi-equilibrium assumption to Eq. [1a], [1c], and [1d] gives rise to the concentrations of the following intermediate and adsorbed species

$$c^2_{M\cdots O} = K_a p_{O_2,o} \quad [7]$$

$$c^2_{MO^-} = K_c c^2_{MOH} c^2_{OH^-,o} \quad [8]$$

$$c^2_{MOH} = K_d c^2_{OH^-,o} \exp\left(\frac{n_d\mathbf{F}}{RT}V\right) \quad [9]$$

where $K_j = k_j/k_{-j}$ for reaction j. Substitution for the above concentrations in Eq. [5] yields

$$i_1 = k_1 c^4_{OH^-,o} \exp\left(\frac{\alpha_{a,1}\mathbf{F}}{RT}V\right) - k_{-1}p_{O_2,o} \exp\left(-\frac{\alpha_{c,1}\mathbf{F}}{RT}V\right) \quad [10]$$

where $\alpha_{a,1} = n_b(\alpha_b + 1)$ and $\alpha_{c,1} = n_b(1 - \alpha_b)$. Note that $n_b = n_d = 2$ and that

$$\alpha_{a,1} + \alpha_{c,1} = 2n_b = n_1 = 4 \quad [11]$$

At equilibrium, $i_1 = 0.0$ and $V = V'_{o,1}$ and therefore the exchange current density corresponding to this surface equilibrium composition is given by

$$i'_{o,1} = k_1 c^4_{OH^-,o} \exp\left(\frac{\alpha_{a,1}\mathbf{F}}{RT}V'_{o,1}\right) = k_{-1}p_{O_2,o} \exp\left(-\frac{\alpha_{c,1}\mathbf{F}}{RT}V'_{o,1}\right) \quad [12]$$

Substitution of Eq. [12] into Eq. [10] yields

$$\frac{i_1}{i'_{o,1}} = \exp\left[\frac{\alpha_{a,1}\mathbf{F}}{RT}(V - V'_{o,1})\right] - \exp\left[-\frac{\alpha_{c,1}\mathbf{F}}{RT}(V - V'_{o,1})\right] \quad [13]$$

An alternate expression for $i'_{o,1}$ can be obtained by eliminating $V'_{o,1}$ from Eq. [12]

$$i'_{o,1} = k_1^{(1-\alpha_{a,1}/n_1)} k_{-1}^{\alpha_{a,1}/n_1} c_{OH^-,o}^{4(1-\alpha_{a,1}/n_1)} p_{O_2,o}^{\alpha_{a,1}/n_2} \quad [14]$$

The rate constants in Eq. [14] are unknown and they can be eliminated by assuming that the exchange current density is known at some reference concentration, $c_{i,ref}$, that is

$$\frac{i'_{o,1}}{i_{o1,ref}} = \left(\frac{c_{OH^-,o}}{c_{OH^-,ref}}\right)^{4(1-\alpha_{a,1}/n_2)} \left(\frac{p_{O_2,o}}{p_{O_2,ref}}\right)^{\alpha_{a,1}/n_1} \quad [15]$$

The open-circuit potential for reaction j evaluated at the surface concentrations, $c_{i,o}$ is defined as

$$V'_{o,j} = U_j^\theta - U_{re}^\theta - \frac{RT}{n\mathbf{F}} \sum_i s_{ij} \ln\left(\frac{c_{i,o}}{\rho_o}\right) + \frac{RT}{n_{re}\mathbf{F}} \sum_i s_{i,re} \ln\left(\frac{c_{i,re}}{\rho_o}\right) \quad [16]$$

when reaction j is written in the form

$$\sum_i s_{ij} M^{z_i} \rightarrow n_j e^- \quad [17]$$

From Eq. [16], the open-circuit potential in terms of reference concentrations, $c_{i,ref}$ is as follows

$$U_{j,ref} = U_j^\theta - 3U_{re}^\theta - \frac{RT}{n\mathbf{F}} \sum_i s_{ij} \ln\left(\frac{c_{i,ref}}{\rho_o}\right) + \frac{RT}{n_{re}\mathbf{F}} \sum_i s_{i,re} \ln\left(\frac{c_{i,re}}{\rho_o}\right) \quad [18]$$

Therefore

$$(V - U_{j,ref}) = V - V'_{o,j} - \frac{RT}{n\mathbf{F}} \sum_i s_{ij} \ln\left(\frac{c_{i,o}}{c_{i,ref}}\right) \quad [19]$$

It is important to note that the ratio of the concentration to the density terms in the logarithmic expressions in the above equations is expressed in units of kg/mol. For dissolved gases such as oxygen, the partial pressure of the gas above the solution appears explicitly in the expression for $U_{j,ref}$ and the ratio of the partial pressure of the gas at the reaction site to the reference partial pressure appears as a multiplier in the expressions for the current density relative to the reference exchange current density. As pointed out by Ryan (16), because these partial pressures appear as ratios at the reaction site, it is reasonable to replace them by the dissolved gas concentration ratio

$$\frac{p_i}{p_{i,ref}} = \frac{c_i}{c_{i,ref}} \quad [20]$$

at all points within the modeled region where the gaseous and liquid phases are in chemical equilibrium.

In terms of reaction [1], the open-circuit potential is given by

$$V - U_{1,ref} = V - V'_{o,1} - \frac{RT}{n_1\mathbf{F}} \ln\left[\left(\frac{p_{O_2,o}}{p_{O_2,ref}}\right)\left(\frac{c_{OH^-,ref}}{c_{OH^-,o}}\right)^4\right] \quad [21]$$

Equations [15] and [21] are substituted into Eq. [13] to obtain the final expression for the current density

$$i_1 = i_{o1,ref}\left[\left(\frac{c_{OH^-,o}}{c_{OH^-,ref}}\right)^4 \exp\left(\frac{\alpha_{a,1}\mathbf{F}}{RT}\eta_1\right) - \left(\frac{c_{O_2,o}}{c_{O_2,ref}}\right) \exp\left(\frac{-\alpha_{c,1}\mathbf{F}}{RT}\eta_1\right)\right] \quad [22]$$

where the overpotential, η_1 is given by

$$\eta_1 = \Phi_{met} - \Phi_o - U_{1,ref} \quad [23]$$

The derivation of the kinetic expressions for the simple reactions in Eq. [2] and [3] follows the approach outlined above for reaction [1]. Mechanistic steps [2b] and [3b] were, respectively, assumed to be the rate-determining steps. The expressions for the final current density terms are given below without going through the rigorous derivation outlined above. For reaction [2]

$$i_2 = i_{o2,ref}\left[\left(\frac{c_{OH^-,o}}{c_{OH^-,ref}}\right)\left(\frac{c_{HO_2^-,o}}{c_{HO_2^-,ref}}\right) \exp\left(\frac{\alpha_{a,2}\mathbf{F}}{RT}\eta_2\right) - \left(\frac{c_{O_2,o}}{c_{O_2,ref}}\right) \exp\left(\frac{-\alpha_{c,2}\mathbf{F}}{RT}\eta_2\right)\right] \quad [24]$$

and for reaction [3]

$$i_3 = i_{o3,ref}\left[\left(\frac{c_{OH^-,o}}{c_{OH^-,ref}}\right)^3 \exp\left(\frac{\alpha_{a,3}\mathbf{F}}{RT}\eta_3\right) - \left(\frac{c_{HO_2^-,o}}{c_{HO_2^-,ref}}\right) \exp\left(\frac{-\alpha_{c,3}\mathbf{F}}{RT}\eta_3\right)\right] \quad [25]$$

where in each case

$$\eta_j = \Phi_{met} - \Phi_o - U_{j,ref} \quad [26]$$

and the sum of the apparent transfer coefficients for reaction j add up to the number of electrons transferred in that reaction, that is

$$\alpha_{a,j} + \alpha_{c,j} = n_j \quad [27]$$

The total current density is equal to the sum of partial current densities as given by

$$i = \sum_{j=1}^{3} i_j \quad [28]$$

The applied potential is defined as

$$E_{appl} = \Phi_{met} - \Phi_{re} \quad [29]$$

and therefore

$$\eta_j = E_{appl} - (\Phi_o - \Phi_{re}) - U_{j,ref} \quad [30]$$

where the potential difference $\Phi_o - \Phi_{re}$ accounts for the ohmic potential drop between the reference electrode and the working electrode.

The common practice in the literature is to report the overall exchange current density instead of the partial exchange current densities. The overall exchange current density is obtained from the equivalent circuit diagram for reactions [1]-[3], in which the resistivity of reaction [1] is in parallel with the sequential resistances of reactions [2] and [3]. The resistances are approximated by linearizing the Butler-Volmer equation for the current density in the vicinity of the open-circuit potential. Therefore, the overall exchange current density for the parallel mechanism (reactions [1]-[3]) is

$$i_{o,ref} = 4i_{o1,ref} + \frac{2i_{o2,ref}i_{o3,ref}}{i_{o2,ref} + i_{o3,ref}} \quad [31]$$

and that for the sequential mechanism (reactions [2] and [3] only) is

$$i_{o,ref} = \frac{2i_{o2,ref}i_{o3,ref}}{i_{o2,ref} + i_{o3,ref}} \quad [32]$$

Kinetic expressions for nonelectrochemical reduction of HO_2^-.—The mechanistic model for this process is given by Eq. [4a]-[4c]. Two cases with different rate controlling steps are considered for this mechanism:

In the first case, reaction [4b] is assumed to be the rate determining step. In this case, the reaction rate equation is given by

$$r_b = k_b c_{MHO_2^-} \quad [33]$$

Assuming that reaction [4a] is in quasi-equilibrium, the equilibrium constant for reaction [4a] is given by

$$K_a = \frac{c_{MHO_2^-}}{c_{HO^-_{2,o}}} \quad [34]$$

Substitution of Eq. [34] into Eq. [33] eliminates $c_{MHO_2^-}$ yielding

$$r_4 = k_h c_{HO^-_{2,o}} \quad [35]$$

where $r_4 = r_b$, and $k_h = k_b K_a$.

For the second case, reaction [4c] is considered as the rds and reactions [4a] and [4b] are assumed to be in quasi-equilibrium. The final rate equation is given by

$$r_4 = k_h (c_{OH^-,o})^{-1} c^2_{HO^-_{2,o}} \quad [36]$$

where $k_h = k_c K_b K_a$.

These two cases are typical of the catalytic decomposition of HO_2^- at electrode surfaces and have been documented extensively in the literature (17-19). For example, on silver electrodes and at low peroxide concentrations, the decomposition of peroxide is found to follow a first-order rate kinetics (17, 18) as shown in Eq. [35]. On the other hand, at high peroxide concentrations, the decomposition of peroxide on silver follows a second-order rate kinetics (19) as shown by the example in Eq. [36].

The rate equations at the electrode surface are related to the rate of transport of reacting species to and from the electrode surface via the material balance equation

$$-N_{i|_{\xi=0}} = \sum_{j=1}^{3} \frac{s_{ij} i_j}{n_j \mathbf{F}} + s_{i4} r_4 \quad [37]$$

The parameters of interest are $i_{oj,ref}$ and $\alpha_{a,j}$ or $\alpha_{c,j}$ and k_h. Estimation of these parameters and analysis of the kinetic data were carried out by the parameter estimation and model discrimination procedure outlined in a previous publication (14). In the analysis of the experimental results, it was assumed that the catalytic decomposition of peroxide on the electrode surface occurred by first-order kinetics.

Experimental Procedure

The rotating disk electrode apparatus was used to collect current/potential data for oxygen reduction on silver. The cell consisted of a silver rotating disk electrode with an area of 0.196 cm^2, a Hg/HgO reference electrode (with a potential of −0.127V measured with respect to a saturated calomel electrode at 25°C) situated in a side compartment, with the end of the Luggin capillary tube positioned directly below and near the silver working electrode, and a platinum counterelectrode located at the bottom of the cell, also directly below the working electrode. A fritted glass tube was provided to bubble the oxygen or nitrogen gas through the solution. The silver working electrode was connected to a variable speed rotator (Pine Instruments Model AFASR) with a maximum speed of 10,000 rpm. The associated electronics apparatus consisted of a potentiostat (Pine Instrument Model AFRDE4) coupled with two digital multiammeters (Hewlett Packard Model 3468A) and an X-Y recorder (Hewlett Packard Model 7015B). A 32% by weight membrane cell grade caustic soda solution (from Dow Chemical Company at Freeport Texas) was used without further purification. This solution was diluted to the desired concentration with triply distilled water. Commercial high purity oxygen and nitrogen gases (Airco purity >99.8%) were used without further purification. Before entering the cell, the gases were presaturated with the solution by passing through the solution of the same concentration. Pretreatment of the rotating disk electrode involved mechanical polishing with alumina powder of grain size 5 and 0.3 μm, respectively. This was followed by degreasing in acetone solution and by repeated washing with distilled water. The electrode was stored in distilled water prior to introduction into the cell.

Table I. Comparison of experimental limiting currents to the diffusion limiting currents calculated from the Levich equation

Ω (rpm)	$I_{L,1}$ (mA)	I_d (Levich) $2e^-$ (mA)	$I_{L,2}$ (mA)	I_d (Levich) $4e^-$ (mA)
400	0.0410	0.024	0.050	0.047
900	0.061	0.035	0.072	0.071
1600	0.073	0.047	0.089	0.094
2500	0.091	0.058	0.108	0.117
3600	0.103	0.071	0.129	0.141

Before each set of polarization measurements was made, the electrode was maintained at a high cathodic potential (−1.0V *vs.* Hg/HgO reference electrode) for about 30s to reduce any surface oxides. This electrode, now referred to as a prereduced electrode, was used to obtain the polarization data.

Measurement of current/potential values was started at the potential of zero current (the open-circuit potential). This was followed by a constant increment in the potential (generally, 0.05V increments) in the cathodic direction. The cell was maintained at each potential for about 30s after which the steady-state current was read. A plot of the current/potential values produced the polarization curve at the specified rotation speed. Polarization curves were first recorded for a nitrogen saturated solution, which in this case served as "blank," to obtain the residual current as a function of the applied potential. The residual currents as a function of the applied potential were very low (typically, <1 μA) and were generally found to be invariable with the rotation speed of the electrode. Oxygen gas was then bubbled through the solution for about 15 min to saturate the solution. A blanket of oxygen was maintained above the solution during measurements by bubbling oxygen at a steady rate through the solution. Current/potential data were collected for oxygen reduction and corrected for the residual current by subtracting the latter at each potential from the corresponding current obtained when O_2 was bubbled through the solution to obtain the polarization data for oxygen reduction. Experimental runs were car-

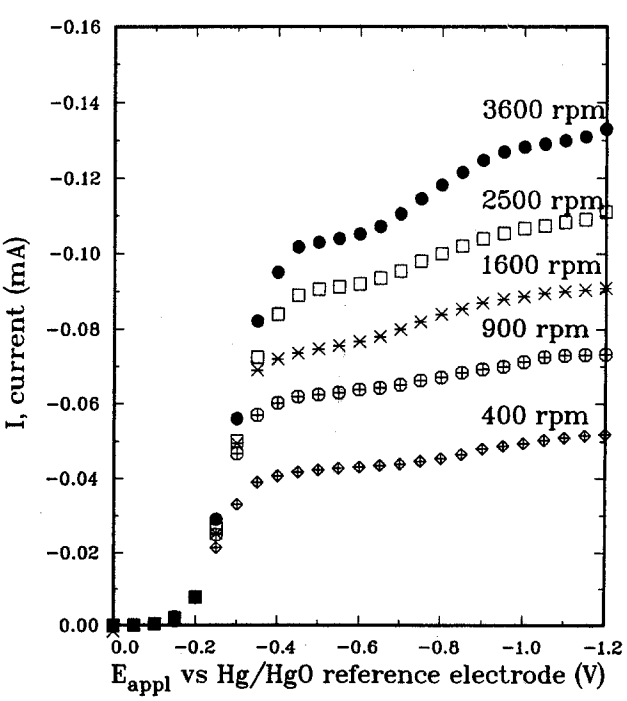

Fig. 1. Polarization data for O_2 reduction on silver in 6.5M NaOH solution.

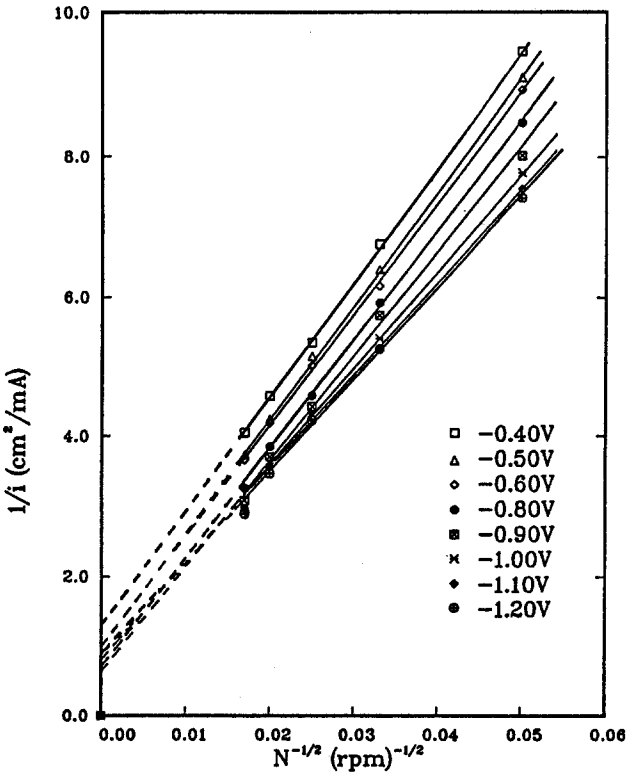

Fig. 2. Plot of $1/i$ vs. $N^{-1/2}$ at various potentials

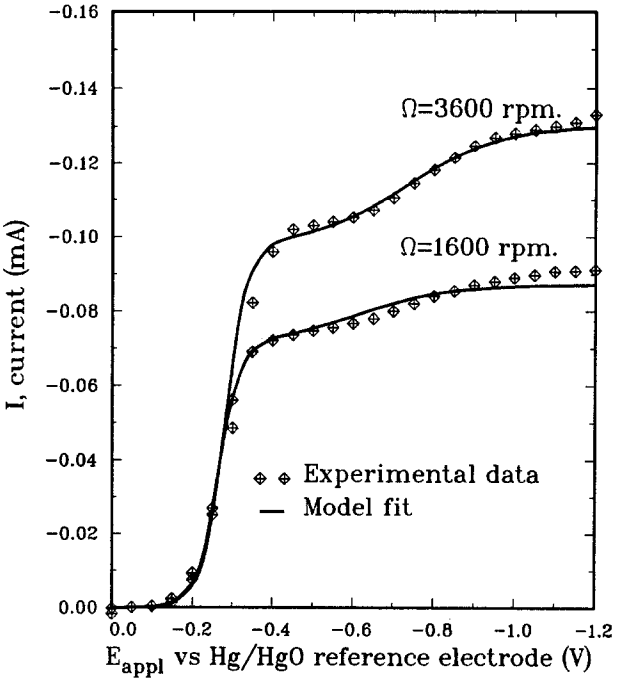

Fig. 3. O_2 reduction on silver in 6.5M NaOH solution. Fit of the parallel mechanism with peroxide decomposition reaction to experimental data.

ried out at a number of rotation speeds (400, 900, 1600, 2500, and 3600 rpm). Figure 1 shows the polarization data for oxygen reduction (corrected for the residual current) in 6.5*M* NaOH solution.

Results and Discussion

The set of data points in Fig. 1 do not exhibit well-defined limiting currents, particularly in the intermediate potential region where the reduction current of oxygen by the $2e^-$ step is expected to approach a limiting value. Yeager *et al.* (5) considered the latter in their case as evidence of the parallel mechanism, that is, the simultaneous participation of the direct $4e^-$ and the two-step $2e^-$ (the sequential) processes for O_2 reduction. However, the occurrence of two apparent limiting currents in the intermediate and higher potential regions suggests that the sequential mechanism might be the dominant process for O_2 reduction in this case. Silver, being a good peroxide decomposition catalyst (1, 2), might also promote catalytic decomposition of peroxide, particularly in the intermediate potential region where the rate of peroxide production is highest. This situation could possibly lead to an enhancement of the limiting current in the intermediate potential region. Table I shows a comparison between the apparent limiting currents from the polarization data to the calculated values from the Levich equation for the $2e^-$ and $4e^-$ processes, respectively. The apparent limiting currents in the intermediate potential region $I_{L,1}$ lie within the upper quartile of the limiting current predicted by the Levich equation for the $4e^-$ process. This indicates an enhancement of the limiting current above the predicted value for the $2e^-$ process. This enhancement might be attributed to either the direct $4e^-$ reaction or the catalytic decomposition of peroxide. However, in the higher potential region, the apparent limiting currents $I_{L,2}$ agree reasonably well with the calculated values for the $4e^-$ process, signifying the reduction of O_2 to OH^- in this region.

The classical technique for analyzing the data in Fig. 1 includes plotting the data according to Eq. [38]

$$\frac{1}{i} = \frac{1}{i_k} + \frac{1}{B\sqrt{N}} \qquad [38]$$

as shown in Fig. 2, where $B = 0.62\, nF D_{O_2}^{2/3} \nu^{-1/6} (2\pi/60)^{1/2} c_{O_2}$. The linearity of these plots indicates that O_2 reduction on Ag in 6.5*M* sodium hydroxide solution is first order with respect to O_2 concentration. The lines are parallel between −0.4 and −0.65V with a slope of 161.8 $cm^2/mA\ (rpm)^{-1/2}$. This slope decreases steadily beyond −0.65V to a value of 135.8 $cm^2/mA\ (rpm)^{-1/2}$ at about −1.0V. The slopes correspond to the value of $1/B$ in Eq. [38], from which the experimental value of B at various potentials can be determined. The value of B at between −0.4 and −0.65V

Table II. Parameter values for analysis of the polarization data for O_2 reduction at Ag electrode in 6.5M NaOH solution

Parameters	Reaction [1]	Reaction [2]	Reaction [3]	Reaction [4]
$\alpha_{c,j}$	0.85	1.00	0.15	
$i_{oj,ref}$ (A/cm²)	10^{-12}	8.0×10^{-8}	10^{-10}	
U_j^{0a} (V)	0.401	−0.0649	0.870	
n_j	4	2	2	
p, k_h (cm/s)				1, 1.30×10^{-2}
Solution properties	O_2	HO_2^-	Na^+	OH^-
$c_{i,ref}$ (mol/cm³)	2.389×10^{-7}	4.264×10^{-9}	0.0065	0.0065
D_i (cm²/s)	7.20×10^{-6}	5.00×10^{-6b}	1.975×10^{-5c}	9.717×10^{-6d}
$A = 0.196$ cm²	$U_{re}^{0} = 0.109$V			
$F = 96487.0$ C/mol	$\rho_o = 0.001$ kg/cm³	$T = 298.15$ K		
$R = 8.314$ J/K-mol	$\nu = 0.0426^d$ cm²/s			

[a]Values taken from (22).
[b]Values taken from (25).
[c]Values taken from (23).
[d]Value taken from (3, 20).

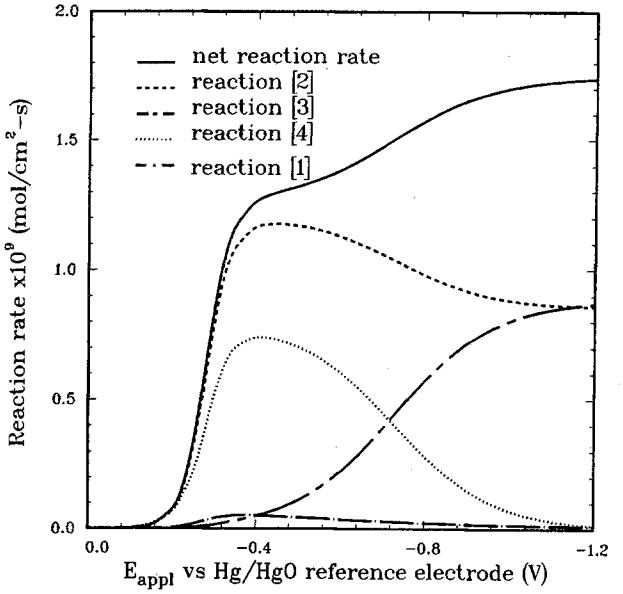

Fig. 4. Plot of partial reaction rates *vs.* E_{appl} at 3600 rpm for the parallel mechanism with peroxide decomposition reaction.

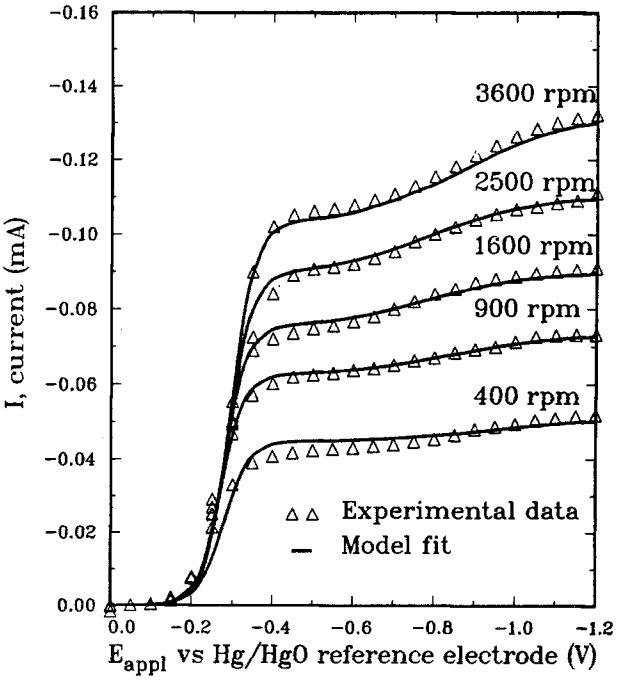

Fig. 5. O_2 reduction on silver in 6.5*M* NaOH solution. Fit of the sequential mechanism with peroxide decomposition reaction to experimental data.

corresponds to 6.180×10^{-3} mA/cm^2 (rpm)$^{1/2}$, compared with the theoretical value of 5.790×10^{-3} mA/cm^2 (rpm)$^{1/2}$. The theoretical value of B was calculated from the Levich equation for $n = 2$ and $\nu = 0.0426$ cm^2/s (20), and using the values of $c_{O_2} = 2.389 \times 10^{-7}$ mol/cm^3 and $D_{O_2} = 7.20 \times 10^{-6}$ cm^2/s from the data of Gubbins *et al.* (21) for O_2 reduction in 21.11 weight percent (w/o) KOH solution (corresponding to 6.5*M* NaOH solution). The experimental B value lying between the calculated values for the $2e^-$ and $4e^-$ processes suggests the reduction of O_2 via the peroxide intermediate step with possibly the catalytic decomposition of peroxide. Plots of $1/i$ *vs.* $1/\sqrt{N}$, at potentials cathodic to -0.7V yield lines with B values that increase steadily up to about -1.0V, approaching the theoretical B value for the $4e^-$ process. Beyond -1.0V, the B values remain constant.

The preceding analysis suggests that the sequential mechanism with catalytic decomposition of peroxide occurs on Ag under the given experimental conditions. The sequential mechanism has also been suggested for O_2 reduction on Pt in 9.2*M* NaOH solution (5). However, previous analysis of kinetic data on O_2 at lower hydroxide concentrations indicates that the parallel mechanism takes place on Ag (8, 11, 14).

Analysis of such complex systems by conventional electrochemical data analysis techniques yields only approximate estimates of some of the parameters and are grossly inadequate in cases where more accurate estimates of the parameters are required. The reason for this is that the participating reactions are coupled with one another over the entire potential range. Attempts to obtain accurate estimates of the parameters requires simultaneous analysis of this system of coupled reactions, a process which is difficult if not impossible with conventional data analysis techniques. The parameter estimation technique presented recently (14) offers a convenient alternative approach for achieving this objective.

Table III. Optimum parameter values for O_2 reduction on Ag in 6.5*M* NaOH

Parameter	Optimum values	Ω = 1600 rpm Relative sensitivity[a]
$i_{o1,ref}$ (A/cm^2)	$(9.641 \pm 0.114) \times 10^{-13}$	0.160
$i_{o2,ref}$ (A/cm^2)	$(8.484 \pm 0.321) \times 10^{-8}$	1.757
$i_{o3,ref}$ (A/cm^2)	$(1.083 \pm 0.182) \times 10^{-10}$	1.318
$\alpha_{c,1}$	0.851 ± 0.013	4.728
$\alpha_{c,2}$	0.910 ± 0.015	38.75
$\alpha_{c,3}$	0.250 ± 0.011	11.79
k_h (cm/s)	$(1.647 \pm 0.278) \times 10^{-2}$	0.921
D_{O_2} (cm^2/s)	$(6.746 \pm 0.019) \times 10^{-6}$	0.640
Parameter	Optimum values	Ω = 3600 rpm Relative sensitivity[a]
$i_{o1,ref}$ (A/cm^2)	$(1.004 \pm 0.31) \times 10^{-12}$	0.208
$i_{o2,ref}$ (A/cm^2)	$(7.668 \pm 0.269) \times 10^{-8}$	2.203
$i_{o3,ref}$ (A/cm^2)	$(2.921 \pm 0.179) \times 10^{-10}$	3.705
$\alpha_{c,1}$	0.850 ± 0.018	3.117
$\alpha_{c,2}$	0.890 ± 0.026	48.68
$\alpha_{c,3}$	0.220 ± 0.023	23.27
k_h (cm/s)	$(1.364 \pm 0.275) \times 10^{-2}$	1.258
D_{O_2} (cm^2/s)	$(6.671 \pm 0.018) \times 10^{-6}$	0.233

[a]See Ref. (14).

From the above analysis, the two most likely mechanisms that could represent the reduction of oxygen on silver in 6.5*M* NaOH are the comprehensive model as given by Eq. [1]-[4] and the sequential mechanism with catalytic decomposition of peroxide as given by Eq. [2]-[4]. First, the comprehensive model was fitted to the data. The initial values for the parameters to be estimated as well as the values of other parameters which must be specified before implementing the optimization procedure (14) are listed in Table II. Figure 3 shows a fit of the comprehensive model to the experimental data at two different rotation speeds, 1600 and 3600 rpm, respectively. The model fits the data reasonably well over nearly the entire range of the polarization curves. In both cases, however, the model shows a moderate deviation from the experimental data beyond -1.0V. This deviation might be due to the onset of the reduction of water to hydrogen, which is not included in the model. The optimum parameter values producing the best fit to the data are presented in Table III. An examination of the values in Table III indicates that the exchange current density for reaction [1] is very small compared to that of reaction [2] or [3]. What this means is that the reduction of O_2 at the electrode surface occurs at a much faster rate by reaction [2] than by reaction [1]. In fact, on the average, reaction [2] is about two to three orders of magnitude faster than reaction [1]. This is confirmed by the magnitudes of the exchange current densities of these two reactions in Table III. This implies that under the given experimental conditions, the sequential mechanism prevails over the direct $4e^-$ mechanism for O_2 reduction on Ag in 6.5*M* NaOH solution. This claim becomes more apparent in Fig. 4 where the individual reaction rates at the optimum values of the parameters are plotted against the applied potential. This figure shows that the oxygen reduction process occurs predominantly via the sequential mechanism with catalytic decomposition of peroxide. The high value of the

Table IV. Optimum parameter values for O_2 reduction on Ag in 6.5M NaOH according to the sequential mechanism with peroxide decomposition

Parameters	Rotation speed (rpm) 400	900	1600	2500	3600
$i_{o2,ref} \times 10^8$	8.156 ± 0.283	9.317 ± 0.332	8.986 + 0.318	9.816 ± 0.329	9.927 ± 0.297
$i_{o3,ref} \times 10^{10}$	2.423 ± 0.178	4.123 ± 0.236	3.844 ± 0.204	4.184 ± 0.245	2.184 ± 0.201
$\alpha_{c,2}$	0.840 ± 0.014	0.902 ± 0.018	0.900 ± 0.016	0.870 ± 0.013	0.856 ± 0.014
$\alpha_{c,3}$	0.178 ± 0.013	0.185 ± 0.015	0.199 ± 0.014	0.198 ± 0.012	0.199 ± 0.013
$k_h \times 10^2$	1.158 ± 0.213	1.357 ± 0.302	1.583 ± 0.287	1.570 ± 0.306	1.524 ± 0.311
$D_{O_2} \times 10^6$	8.438 ± 0.025	7.908 ± 0.021	6.948 ± 0.021	6.747 ± 0.019	6.893 ± 0.022

catalytic decomposition rate constant, k_h, shows that a substantial proportion of the peroxide formed undergoes catalytic decomposition at the electrode surface, particularly at potentials anodic to −0.6V, before the electrolytic reduction of peroxide by reaction [3] becomes competitive at the more negative potentials. This is confirmed again in Fig. 4 where the catalytic peroxide decomposition rate increases to a maximum value of about two orders of magnitude greater than the corresponding electrolytic peroxide reduction rate in the potential region of −0.3 to −0.6V. Thereafter, the catalytic decomposition rate decreases very rapidly in the potential range beyond −0.60V, the region in which the electrolytic decomposition rate becomes more favorable. Between −0.3 to−0.6V, the regeneration of oxygen by catalytic decomposition of peroxide in reaction [4] leads to an enhancement in the peroxide production rate by reaction [2]. At such high k_h values, the regenerative reaction in Eq. [4] enhances the limiting current of the $2e^-$ step for O_2 reduction by reaction [2] to that approaching the direct $4e^-$ process in reaction [1] [see Fig. 2 in Ref. (24)].

Sensitivity analysis of the parameters (Table III) shows the apparent transfer coefficients, particularly $\alpha_{c,2}$ and $\alpha_{c,3}$, to be the most sensitive parameters. The least sensitive are $i_{o1,ref}$ and D_{O_2}.

The preceding analysis indicates that the sequential mechanism with catalytic decomposition of peroxide should be sufficient to describe the data. Therefore, this sequential mechanism was fitted to the data next. The results are displayed in Fig. 5. The model fits the data reasonably well over nearly all the rotation rates. However, moderate deviations between the predicted and experimental curves are observed in the intermediate potential regions at the lower rotation rates (of 400 and 900 rpm, respectively). The optimum parameter values for the best model fit at each rotation speed are given in Table IV. Finally, the sequential mechanism was fitted to all the data pooled over all five rotation speeds (400, 900, 1600, 2500, and 3600 rpm) in order to determine the average optimum parameter values for the entire data set. For the pooled data, the objective function, F, to be minimized is a summation of the residual error between the predicted and observed values over the entire potential range and over all the rotation speeds at which the data are collected, as defined by Eq. [39]

$$F(x, t) = \sum_{l=1}^{n_w} \sum_{k=1}^{n} w_{k,l}[y_{k,l,obs} - f_{k,l}(x, t)]^2 \quad [39]$$

The objective function in Eq. [39] was subjected to the optimization procedure (14) to give the pooled parameter estimates and their confidence limits as shown in Table V. Plots of the predicted current/potential curves using these parameter values for the various rotation speeds are shown in Fig. 6. A comparison of some parameter values in Table V to available literature values is shown in Table VI. A striking point to note about the parameter values for O_2 reduction on Ag in 6.5M NaOH solution as presented here and in 0.127N KOH solution as discussed previously [see Ref. (14)] is the difference in the reference exchange current density for reaction [1], the direct $4e^-$ process for O_2 reduction. While the reference exchange current densities for the other reactions and the apparent transfer coefficients compare favorably for the two cases, $i_{o1,ref}$ for O_2 reduction in 6.5M is approximately two orders of magnitude less than the corresponding value in 0.127N KOH solution. This difference in reaction rates of the $4e^-$ process is most likely responsible for the variation in mechanism for the two cases under comparison. In 0.127N KOH solution, because of the higher rate of reaction [1], the parallel mechanism with the direct $4e^-$ process dominating in the lower to intermediate potential regions tends to be favored. On the other hand, in 6.5M NaOH solution, the rate of reaction [1] is much smaller compared to the sequential step in reaction [2]. Consequently, the sequential mechanism appears to be more favorable for this case. Comparison of the overall exchange current densities shows a one to two orders of magnitude increase in value from 6.5M NaOH solution to the more dilute 0.1M KOH solution. While the increase in the exchange current density can be attributed partly to the differences in oxygen solubility in the two solutions, a comparison of the equations for the exchange current densities for the two cases indicates that the surface electrode reactions might play a more significant role in this respect. A comparison of the other parameters shows that the diffusion coefficient for oxygen in 6.5M NaOH compares favorably with the value of Gubbins *et al.* (21) for O_2 in 21.11 w/o KOH solution. Also, the k_h value for the catalytic decomposition of HO_2^- in 6.5M NaOH solution compares reasonably well with the value obtained by analysis of the

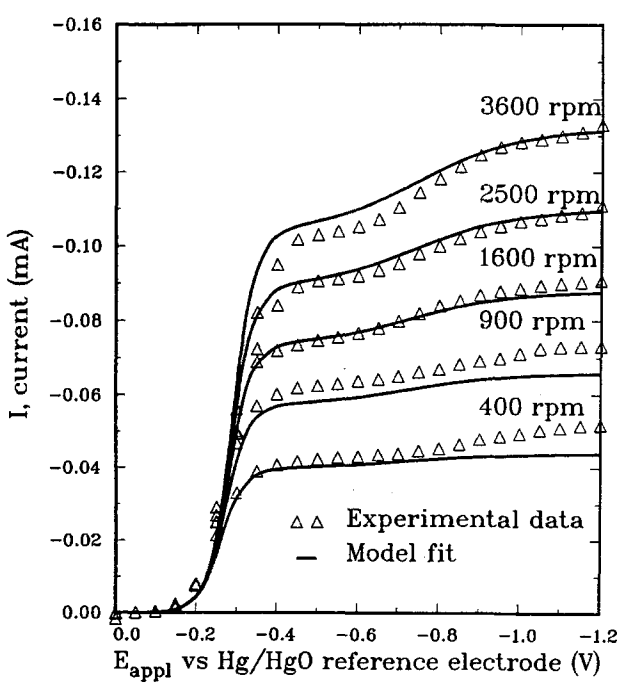

Fig. 6. Fit of the sequential mechanism with peroxide decomposition reaction to experimental data using average optimum parameter estimates pooled over all five rotation speeds.

Table V. Pooled parameter values for O_2 reduction on Ag in 6.5M NaOH solution

Parameter	Value
$i_{o2,ref}$ (A/cm^2)	(8.156 ± 0.274) × 10^{-8}
$i_{o3,ref}$ (A/cm^2)	(4.123 ± 0.306) × 10^{-10}
$\alpha_{c,2}$	0.902 ± 0.024
$\alpha_{c,3}$	0.206 ± 0.033
k_h (cm/s)	(1.571 ± 0.281) × 10^{-2}
D_{O_2} (cm^2/s)	(6.708 ± 0.063) × 10^{-6}

Table VI. Comparison of parameter estimates of D_{O_2} and k_h to literature values

Parameter	This analysis[a]	This analysis[b]	Brezina *et al.*[c]	Literature values
$i_{o1,ref} \times 10^{10}$	—	0.010	2.856	
$i_{o2,ref} \times 10^{8}$	8.156	7.668	2.211	
$i_{o3,ref} \times 10^{10}$	4.123	2.921	0.937	
$i_{o,ref} \times 10^{9}$	40.821	0.587	1.287	200.0[d]
$\alpha_{c,1}$	—	0.850	0.780	
$\alpha_{c,2}$	0.902	0.890	1.010	
$\alpha_{c,3}$	0.206	0.220	0.149	
$k_h \times 10^{2}$	1.571	1.364	1.00	1.00[e]
$D_{O_2} \times 10^{6}$	6.708	6.671	1.904	7.241[f]

[a]Sequential mechanism with catalytic decomposition of peroxide.
[b]Comprehensive mechanism at 3600 rpm.
[c]In 0.127*N* KOH solution [see Ref. (13)].
[d]In 0.1*M* KOH solution (11).
[e]In 0.1*M* KOH solution (18).
[f]From Gubbins *et al.* in 21.11 w/o KOH solution (21).

data of Brezina *et al.* (13) in 0.127*N* KOH, as well as the value obtained by Merkulova *et al.* (18) in 0.1*N* KOH.

Conclusion

Kinetic analysis of the data presented for oxygen reduction on silver in 6.5*M* NaOH solution indicates that the parallel mechanism in which the sequential pathway dominates the direct $4e^-$ pathway prevails on silver under the given experimental conditions. As a consequence of this, the reduction process can conveniently be described by the sequential mechanism. The peroxide intermediate formed undergoes significant catalytic decomposition in the potential range in which peroxide is produced, confirming the role of silver as a good peroxide decomposition catalyst.

Acknowledgment

The authors wish to express their gratitude to Dow Chemical Company (in Freeport, Texas) for supplying the membrane-grade caustic soda used in this work.

Manuscript submitted Sept. 9, 1987; revised manuscript received Feb. 27, 1988.

Texas A&M University assisted in meeting the publication costs of this article.

LIST OF SYMBOLS

A surface area of electrode, cm^2
B Levich constant defined in Eq. [38]
c_i concentration of species i, mol/cm^3
D_i diffusion coefficient of species i, cm^2/s
E_{appl} applied electrode potential, V
$\mathbf{F}$ Faraday's constant, 96,487 C/mol
$F(x, t)$ objective function
$f_{k,l}$ k^{th} predicted value of dependent variable at lth rotation rate
i total current density, A/cm^2
i_j local current density due to reaction j, A/cm^2
i_k current density in the absence of mass transport, A/cm^2
$i_{oj,ref}$ exchange current density due to reaction j at reference concentrations, A/cm^2
$i_{o,ref}$ overall exchange current density at reference concentrations, A/cm^2
I total current, A
$I_{L,j}$ limiting current of reaction j, A
I_d diffusion limiting current obtained from the Levich equation, A
k_h rate constant for noncharge transfer reaction at electrode surface
N rotation speed, rpm
N_i flux of species i, mol/cm^2-s
n_j number of electrons transferred in reaction j
n_w number of rotation rates
p reaction order with respect to peroxide concentration in catalytic rate equation for peroxide decomposition
R universal gas constant, 8.314 J/mol-K
rpm revolution per minute
t independent variable
T absolute temperature, K
U_j^θ standard electrode potential for reaction j, V
U_{re}^θ standard potential of the reference electrode on the hydrogen electrode scale, V
$w_{k,l}$ weight attached to the k^{th} observed value at the l^{th} rotation rate
$\mathbf{x}$ parameter vector
$y_{k,l}$ the k^{th} observed value of dependent variable at the l^{th} rotation rate

Greek

$\alpha_{a,j}$ anodic transfer coefficient for reaction j
$\alpha_{c,j}$ cathodic transfer coefficient for reaction j
ρ_o pure solvent density, kg/cm^3
ν kinematic viscosity, cm^2/s
Ω rotation speed, rad/s

Subscripts

o at the electrode surface
j reaction j
re reference electrode
ref reference conditions
bulk in the bulk solution

REFERENCES

1. A. G. Kicheev, S. B. Kalmykova, Yu. A. Kvashnin, V. N. Saleva, and G. N. Maksimov, *Soviet Electrochem.*, **21,** 846 (1985).
2. E. L. Littauer and K. S. Tsai, *This Journal*, **126,** 1924 (1979).
3. A. Liebhasfsky and E. J. Cairns, "Fuel Cells and Fuel Batteries," John Wiley and Sons, Inc., New York (1968).
4. A. Gibney and D. Zuckerbrod, in "Power Sources," Vol. 9, J. Thompson, Editor, p. 143, Academic Press, Inc., London (1983).
5. E. B. Yeager, U.S. Dept. of Energy Contract, EC-77-C-02-4146, Annual Report, Oct. 1977-Sept. 1978.
6. G. Bianchi, G. Caprioglio, F. Mazza, and T. Mussini, *Electrochim. Acta*, **4,** 232 (1961).
7. S. Z. Beer and Y. L. Sandler, *This Journal*, **112,** 1133 (1965).
8. N. A. Shumilova, G. V. Zhutaeva, and M. T. Tarasevich, *Electrochim. Acta.*, **11,** 967 (1966).
9. T. Hurlen, Y. L. Sandler, and E. A. Pantier, *ibid.*, **11,** 1463 (1966).
10. D. B. Sepa, M. V. Vojnovic, and A. Damjanovic, *ibid.*, **15,** 1355 (1970).
11. P. Fischer and J. Heitbaum, *J. Electroanal. Chem.*, **112,** 281 (1980).
12. C. Fabjan, M. R. Kazemi, and A. Neckel, *Ber. Bunsenges. Phys. Chem.*, **84,** 1026 (1980).
13. M. Brezina, J. Koryta, and M. Musilova, *Collect. Czech. Chem. Commun.*, **33,** 3397 (1968).
14. P. K. Adanuvor and R. E. White, *This Journal*, **135,** 1887 (1988).
15. B. Case, *Electrochim. Acta*, **18,** 293 (1973).
16. W. E. Ryan, M.S. Thesis, Texas A&M University, College Station, TX (1986).
17. M. Brezina and J. Phuong, *J. Electroanal. Chem.*, **40,** 107 (1972).
18. N. D. Mekulova, G. V. Zhutaeva, N. A. Shumilova, and M. R. Tarasevich, *ibid.*, **18,** 169 (1973).
19. K. Goszner, D. Korner, and R. Hite, *J. Catal.*, **25,** 245 (1972).
20. A. V. Wolfe, M. G. Brown, and P. G. Prentiss, in "CRC Handbook of Chemistry and Physics," 63rd ed., R. C. Weast, Editor, p. D227, CRC Press, Inc., Boca Raton,

FL (1982).
21. K. E. Gubbins and D. Walker, *This Journal*, **112**, 469 (1965).
22. J. P. Hoare, in "Standard Potentials in Aqueous Solution," A. J. Bard, R. Parson, and J. Jordan, Editors, Marcel Dekker, Inc., New York (1985).
23. J. S. Newman, "Electrochemical Systems," Prentice-Hall, Inc., Englewood Cliffs, NJ (1973).
24. P. K. Adanuvor and R. E. White, *This Journal*, **134**, 1093 (1987).
25. E. L. Littauer and K.C. Tsai, *Electrochim. Acta*, **24**, 681 (1979).

An Ellipsometric Study of the Nucleation and Growth of Polythiophene Films

Andrew Hamnett

Inorganic Chemistry Laboratory, University of Oxford, Oxford, England, OX1 3QR

A. Robert Hillman*

School of Chemistry, University of Bristol, Bristol, England, BS8 1TS

ABSTRACT

The electrodeposition of polythiophene films has been monitored ellipsometrically. The species that are generated immediately after application of the polymerization potential form in solution near the electrode. Deposition of material on the electrode commences a short time later, in agreement with the point at which current-time data indicate nucleation of growth sites. Previous analysis of current-time data suggested three-dimensional growth, but calculation of film thickness as a function of time from ellipsometric data shows that the process is more complex. Films formed at different potentials require different thicknesses of polymer to be deposited before the film properties approach those characteristic of the bulk film. There is, furthermore, a marked distinction between the optical properties of films as grown at potentials above and below approximately 2.0V. The presence of excess water in the polymerization solution results in the production of a film about 1.5 nm thick which is optically dissimilar from that produced in the absence of water.

The electronic and optical properties of conducting polymers have received considerable attention owing to their potential application in electronic and optical devices (1-3). Optimization of such devices demands a thorough understanding of these materials. Central to success in this endeavor is control of physical properties, both within a given system, for example via the electrode potential, and between systems, for example by substitution. The system we have been studying and on which we now report new data is polythiophene. Recently we have published an electrochemical study of the nucleation and growth of these films as a function of potential (4). In that work, which followed that of Pletcher on the related polypyrrole (5) and poly-N-methylpyrrole (6) systems, we deduced that growth occurs in a three-dimensional fashion and that overlap of the growing centers occurs quite rapidly. We were also able to place estimates on kinetic parameters for film growth as functions of the polymerization potential.

Since purely electrochemical information is unable to identify species produced, except in an indirect manner, we have also elected to employ spectroscopic methods. These are frequently less quantitative, but do have the complementary feature that they supply structural information directly. In a separate report (7) we have described the use of time-resolved UV-visible spectroscopy to monitor intermediates and products during the electrochemical polymerization of thiophene. Those measurements were made in transmission mode, so that experiment-detected species both on the electrode surface and in the solution: the detection of both types of species is on the one hand an advantage and on the other hand a source of ambiguity. We therefore turned to ellipsometry which is, by its very nature, surface specific. The sensitivity and diagnostic power of this technique has been demonstrated in a preliminary report describing the growth of polymeric films derived from thionine (8, 9) and from thiophene at high potentials (10). Here we present more detailed studies of the polythiophene deposition process at less positive potentials consistent with the more highly controlled conditions under which our nucleation studies were performed. A more detailed comparison of data from ellipsometry and UV-visible transmission spectroscopy will be presented elsewhere, but we show here briefly how powerful this combination can be, and how reliance on purely electrochemical data can result in failure to perceive some of the more complex and subtle features of electrochemical film deposition.

*Electrochemical Society Active Members.

Experimental

Full details of the ellipsometric apparatus have been given elsewhere (11). It comprises a Rudolph Instruments RR2000 automatic ellipsometer interfaced to a Matmos Z-80 based microcomputer. The equipment has a basic sampling time of *ca.* 0.02s, but possesses the ability to average 10 or 100 data points, giving sampling times of 0.2 or 2s. The light sources were a 5 mW He-Ne laser and a Xe lamp with appropriate interference filters. The computer was also used to control the purpose-built potentiostat system. Current-time transients were captured on an oscilloscope (Gould OS4000) and output to an X-Y-t recorder (Gould-Bryans 60,000 Series) or directly on the recorder, as appropriate to the time scale.

Thin films of Pt or Au (~100 nm) sputtered on glass were used as working electrodes. A Pt gauze was used as the counterelectrode. All potentials were measured, and are quoted, with respect to a saturated calomel electrode; this was separated from the main cell compartment by a salt bridge to prevent undue contamination with water.

The background electrolyte was 0.1 mol dm^{-3} tetraethylammonium-tetrafluoroborate, TEAT, (puriss., Fluka) in acetonitrile (Analar), which had previously been refluxed over CaH_2, distilled, and stored over molecular sieves. Thiophene was added via a syringe to solutions used for polymerization in sufficient quantities to bring the monomer concentration to 10 mmol dm^{-3}. Polymerization was performed by a double potential step from 0 V to the polymerization potential, $1.75 < E_{pol}/V < 1.90$, and back to 0 V. All solutions were purged with dry nitrogen, but the gas stream was directed over the solution during data acquisition to ensure quiescent solution conditions. Measurements were made at room temperature, 20° ± 2°C. Although the results of potential cycling are not described here, cyclic voltammograms were run after each polymerization run as a routine quality control check.